ORGANOMETALLICS

Article

pubs.acs.org/Organometallics

Yttrium and Aluminum Alkyl Complexes of a Rigid Bis-Anilido NON-Donor Ligand: Synthesis and Hydroamination Catalysis

Kelly S. A. Motolko, David J. H. Emslie,* and Hilary A. Jenkins

Department of Chemistry, McMaster University, 1280 Main Street West, Hamilton, Ontario L8S 4M1, Canada

Supporting Information

ABSTRACT: The palladium-catalyzed coupling of 4,5-dibromo-2,7-di-*tert*-butyl-9,9-dimethylxanthene (XBr_2) with 2 equiv of 2,4,6-triisopropylaniline afforded the proligand 4,5-bis(2,4,6-triisopropylanilino)-2,7-di-*tert*-butyl-9,9-dimethylxanthene (H_2XN_2), and reaction of H_2XN_2 with $[Y(CH_2SiMe_2R)_3(THF)_2]$ (R = Me, Ph) produced the monoalkyl yttrium complexes $[(XN_2)Y(CH_2SiMe_2R)(THF)]$ (R = Me (**1a**), Ph (**1b**)). Neutral **1a** showed near-zero ethylene polymerization activity (1 atm, 20 and 80 °C), and in the presence of $AlMe_3$, **1a** converted to $[(XN_2)Y\{(\mu\text{-}Me)_2AlMe_2\}(THF)]$ (**2**). Compound **2** is thermally robust, and transfer of the XN_2 ligand from yttrium to aluminum was not observed even at elevated temperatures. However, $[(XN_2)AlMe]$ (**3**) was accessible via the reaction of H_2XN_2 with $AlMe_3$, demonstrating the ability of the wide-bite-angle XN_2 ligand to coordinate to much smaller aluminum(III). Neutral **1a** proved to be highly active for both intra- and intermolecular hydroamination with various substrates, yielding Markovnikov products in the intermolecular hydroamination reactions with 1-octene.

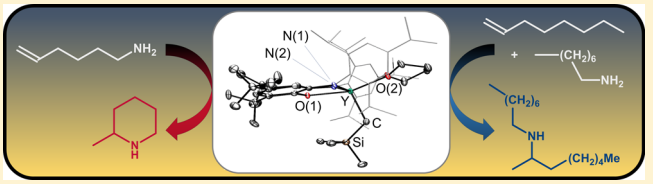

INTRODUCTION

Group 3 transition metal and f-element complexes are among the most active catalysts for intramolecular alkene hydroamination. In contrast, intermolecular hydroamination of unactivated alkenes remains particularly challenging, and only a handful of electropositive metal complexes show high catalytic activity.[1] These catalysts include rare-earth *ansa*-cyclopentadienyl and 1,1′-binaphthalene backbone ligand complexes developed by Marks[2] and Hultzsch,[3,4] respectively (Figure 1;

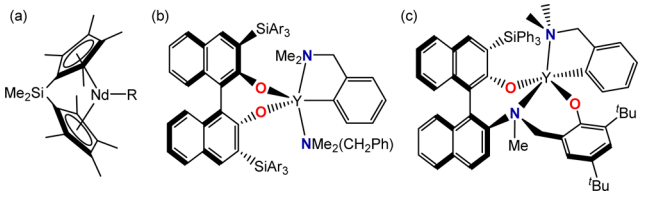

Figure 1. State of the art rare-earth catalysts for intermolecular hydroamination of unactivated alkenes (R = $CH(SiMe_3)_2$).

Ar = Ph). The majority of hydroamination catalysts are neutral, whereas most olefin polymerization catalysts are cationic,[5,6] capitalizing on lower coordination numbers and more electrophilic metal centers. Nevertheless, a small number of highly[5] active neutral (i.e., single-component) rare-earth alkyl ethylene polymerization catalysts have been reported, including the alkyl yttrocene[7] and samarium tetramethylaluminate[8] complexes in Figure 2.

For both alkene/alkyne hydroamination and olefin polymerization, catalytic activity is highly sensitive to the steric and electronic properties of the supporting ligand(s). For example, the rate of 1-amino-2,2-dimethyl-4-pentene cyclization by

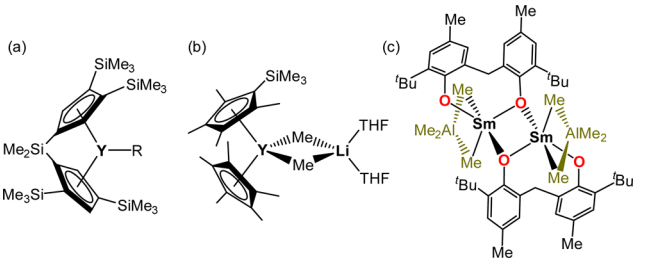

Figure 2. Highly active single-component rare-earth catalysts for ethylene polymerization (R = $CH(SiMe_3)_2$).

$[(L)Lu\{CH(SiMe_3)_2\}]$ catalysts increased substantially as the ligand set, L, was varied from two C_5Me_5 (Cp*) anions to $Me_2Si(C_5Me_4)_2$ to $Me_2Si(C_5Me_5)(N^tBu)$.[9] Furthermore, the supporting ligand set plays a critical role in defining the temperature range within which a catalyst can operate.

Previous research in the Emslie group explored the potential for the highly rigid, dianionic pincer ligand 4,5-bis(2,6-diisopropylanilido)-2,7-di-*tert*-butyl-9,9-dimethylxanthene (XA_2) to provide access to actinide(IV) alkyl complexes with high thermal stability and reactivity. This led to the synthesis and isolation of neutral $[(XA_2)An(CH_2R)_2]$ (An = Th, R = $SiMe_3$, Ph;[10] An = U, R = $SiMe_3$, CMe_3) complexes, which decomposed only slowly at 80 °C (R = $SiMe_3$). Furthermore, reactions of $[(XA_2)Th(CH_2R)_2]$ (R = $SiMe_3$, Ph) with $[CPh_3][B(C_6F_5)_4]$ afforded the first examples of non-cyclopentadienyl thorium alkyl cations, $[(XA_2)Th(CH_2SiMe_3)(\eta^n\text{-arene})][B(C_6F_5)_4]$ (arene = benzene, toluene; Figure 3) and

Received: February 27, 2017

DOI: 10.1021/acs.organomet.7b00156
Organometallics XXXX, XXX, XXX−XXX

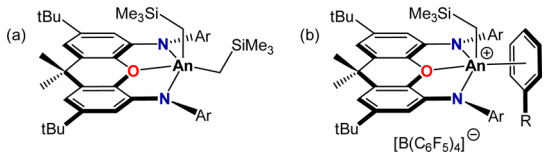

Figure 3. Actinide(IV) alkyl complexes of the XA_2 pincer ligand: (a) neutral $[(XA_2)An(CH_2SiMe_3)_2]$; (b) cationic $[(XA_2)An(CH_2SiMe_3)(\eta^n\text{-arene})][B(C_6F_5)_4]$ (An = Th, U; Ar = 2,6-diisopropylphenyl; R = H, Me, F).

$[(XA_2)Th(CH_2Ph)(\eta^n\text{-toluene})][B(C_6F_5)_4]$.[12] However, in toluene and benzene, these thorium alkyl cations were inactive for ethylene (1 atm) polymerization, likely due to an inability of ethylene to compete with the arene solvents for coordination to thorium.

Following on from this research, we became interested to determine whether 4,5-bis(anilido)xanthene ligands (i.e., XA_2 and related rigid pincer ligand dianions) could provide access to thermally robust monoalkyl complexes of trivalent rare-earth elements and whether these neutral complexes would exhibit appreciable activity for olefin polymerization or alkene/alkyne hydroamination; alkyl complexes with high thermal stability are of particular interest for intermolecular hydroamination, since this challenging transformation typically requires extended reaction times at elevated temperature.

Herein we report the synthesis of thermally robust yttrium monoalkyl and tetramethylaluminate complexes of a 4,5-bis(anilido)xanthene pincer ligand that is closely related to XA_2, isolation of a base-free aluminum methyl analogue, and both intra- and intermolecular hydroamination using the yttrium trimethylsilylmethyl complex.

RESULTS AND DISCUSSION

Hartwig–Buchwald coupling of 4,5-dibromo-2,7-di-*tert*-butyl-9,9-dimethylxanthene (XBr_2)[13] with 2 equiv of 2,4,6-triisopropylaniline[14] afforded the proligand 4,5-bis(2,4,6-triisopropylanilino)-2,7-di-*tert*-butyl-9,9-dimethylxanthene (H_2XN_2) in a 52% isolated yield. The XN_2 dianion is closely related to the previously reported XA_2 dianion (vide supra), and reaction of H_2XN_2 with $[Y(CH_2SiMe_2R)_3(THF)_2]$ (R = Me, Ph),[15] followed by crystallization from $O(SiMe_3)_2$, afforded the monoalkyl yttrium complexes $[(XN_2)Y(CH_2SiMe_2R)(THF)]\cdot xO(SiMe_3)_2$ (R = Me (**1a**·$xO(SiMe_3)_2$; x = 1.0–1.5), Ph (**1b**·$O(SiMe_3)_2$; x = 1.0)) (Scheme 1). **1a**,**b** are both only ~50% decomposed after 12 h at 100 °C, demonstrating appreciable thermal stability.

The ^{1}H NMR spectra of **1a**,**b** are consistent with the expected C_s-symmetric structures, as evidenced by two Ar-*H*, two *o*-C*H*Me_2, and two C*Me*$_2$ peaks, and in both compounds the yttrium-C*H*$_2$ signal was observed as a low-frequency doublet (−0.22 and −0.07 ppm, respectively); the $^2J_{^1H,^{89}Y}$ coupling is 3.5 Hz, which is slightly above the usual range of 1.8–2.8 Hz.[16] X-ray-quality crystals of **1a**·$O(SiMe_3)_2$ (Figure 4)

Scheme 1. Synthesis of Yttrium Complexes 1a (R = Me) and 1b (R = Ph) from $[YR'_3(THF)_2]$ (R′ = CH_2SiMe_2R)

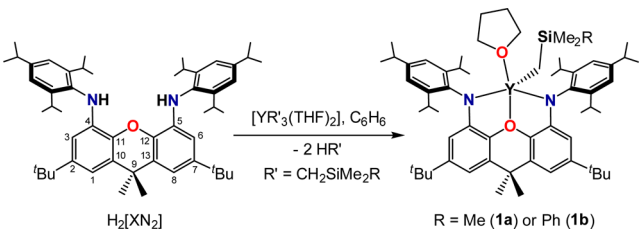

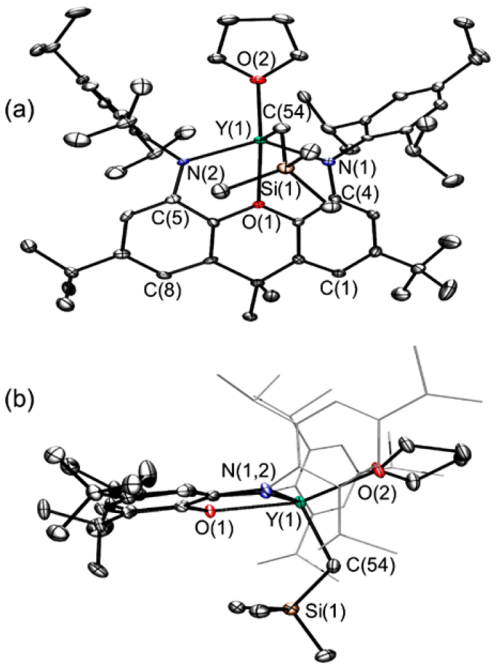

Figure 4. Two views of the X-ray crystal structure for $[(XN_2)Y(CH_2SiMe_3)(THF)]\cdot O(SiMe_3)_2$ (**1a**·$O(SiMe_3)_2$). Ellipsoids are set to 50% probability. Hydrogen atoms and lattice solvent are omitted, and in (b) the 2,4,6-triisopropylphenyl groups are depicted in wire-frame format for clarity. Selected bond lengths (Å) and angles (deg): Y–N(1) 2.252(3), Y–N(2) 2.252(3), Y–C(54) 2.364(3), Y–O(1) 2.347(2), Y–O(2) 2.312(2); N(1)–Y–N(2) 128.88(9), N(1)–Y–C(54) 105.9(1), N(2)–Y–C(54) 109.9(1), O(1)–Y–C(54) 103.98(9), O(2)–Y–C(54) 97.4(1), O(2)–Y–N(2) 106.62(8), O(2)–Y–N(1) 103.60(9), Y–C–Si 121.3(2).

were obtained by cooling a concentrated $O(SiMe_3)_2$ solution to −30 °C. Yttrium is five-coordinate with the three anionic donors and THF arranged in an approximate tetrahedron around the metal center. The smallest angle in this distorted tetrahedron is the O(2)–Y–C(54) angle of 97°, and the largest angle is the N(1)–Y–N(2) angle of 129°, while the others are between 104 and 110°. The central oxygen donor of the xanthene backbone is coordinated on the N(1)/N(2)/C(54) face of the tetrahedron, closest to the nitrogen donors, with 68–69° N(1)–Y–O(1) and N(2)–Y–O(1) angles. Yttrium lies 0.74 Å out of the plane of the XN_2 ligand donor atoms, leading to a 50° angle between the NON plane and the NYN plane. The xanthene backbone of the XN_2 ligand is slightly bent, with a 25° angle away from planarity, on the basis of the relative orientation of the two aryl rings of the ligand backbone. Additionally, in order to accommodate yttrium within the coordination pocket of the ligand, the nitrogen donors of the ligand are bent toward the metal, as illustrated by C(1)···C(8), C(4)···C(5), and N(1)···N(2) distances of 4.98, 4.56, and 4.06 Å, respectively.

The Y–N distances of 2.252(3) Å in **1a** are within the expected range in comparison to those in related yttrium compounds, including $[(O\{C_6H_4(N^tBu)\text{-}o\}_2)Y\{CH(SiMe_3)_2\}(THF)]$ (2.294(9) and 2.286(10) Å),[17] $[\{(R)\text{-}C_{20}H_{12}(NSiMe_3)_2\}Y(CH_2SiMe_3)(THF)_2]$ (2.254(3) and

DOI: 10.1021/acs.organomet.7b00156
Organometallics XXXX, XXX, XXX–XXX

2.278(3) Å),[18] and [{ArN(CH$_2$)$_3$NAr}Y(CH$_2$Ph)(THF)$_2$] (Ar = C$_6$H$_3$^{i}Pr$_2$-2,6; 2.215(4) and 2.191(3) Å).[19] Additionally, the Y−O$_{THF}$ and Y−O(1) distances (2.312(2) and 2.347(2) Å, respectively) are unremarkable and are similar to those in [(O{C$_6$H$_4$(N^{t}Bu)-*o*}$_2$)Y{CH(SiMe$_3$)$_2$}(THF)] (Y−O$_{THF}$ = 2.356(8) Å, Y−O$_{OAr2}$ = 2.337(8) Å).[17] The Y−C(54) distance is 2.364(3) Å, which falls at the lower end of the range typically observed for five-coordinate yttrium alkyl compounds such as [{(*R*)-C$_{20}$H$_{12}$(NSiMe$_3$)$_2$}Y(CH$_2$SiMe$_3$)(THF)$_2$] (2.434(4) Å),[18] [{(*Z*)-ArNC(Me)=C(Me)NAr}Y(CH$_2$SiMe$_3$)(THF)$_2$] (Ar = C$_6$H$_3$^{i}Pr$_2$; 2.399(2) Å),[20] and [{ArNCMeCHCMeN-(CH$_2$)$_2$N^{t}Bu}Y(CH$_2$SiMe$_3$)(THF)] (2.377(3) Å).[21]

The neutral monoalkyl complex **1a** was tested for ethylene polymerization catalysis at 20 and 80 °C for 1 h (toluene, 1 atm of ethylene) but showed near-zero activity. The potential for **1a** to polymerize 1-octene was also evaluated, with and without the addition of Al(octyl)$_3$ (20 equiv) to act as a scavenger for residual moisture or reactive impurities, and again no polymer formation was observed. However, a ^{1}H NMR spectrum of **1a** in the presence of Al(octyl)$_3$ or AlMe$_3$ revealed the formation of a new yttrium complex, and [(XN$_2$)Y{(μ-Me)$_2$AlMe$_2$}-(THF)]·O(SiMe$_3$)$_2$ (**2**·O(SiMe$_3$)$_2$) was isolated from the reaction of **1a** with excess AlMe$_3$ (Scheme 2), followed by

Scheme 2. Reaction of Yttrium Alkyl Complex 1a with Excess AlMe$_3$ To Form [(XN$_2$)Y{(μ-Me)$_2$AlMe$_2$}(THF)] (2)

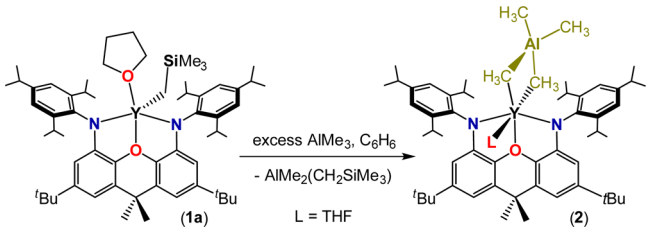

crystallization from O(SiMe$_3$)$_2$. Compound **2** is C_s symmetric, featuring a doublet at −0.56 ppm ($^2J_{^1H,^{89}Y}$ = 3.8 Hz) for the 12 Al*Me*$_4$ protons in the ^{1}H NMR spectrum, indicative of rapidly exchanging terminal and bridging methyl groups at room temperature; similar behavior has previously been reported by Anwander et al. for [{HC(NAr)$_2$}Y(AlMe$_4$)$_2$][22] and [{N-(NC$_6$H$_4$Ar-*o*)$_2$}Y(AlMe$_4$)$_2$] (Ar = C$_6$H$_3$^{i}Pr$_2$-2,6),[23] [(BDPP)Y-(AlMe$_4$)] (BDPP = 2,6-bis(2,6-diisopropylanilidomethyl)-pyridine),[24] and [{(AlMe$_4$)Y(μ-N(C$_6$H$_2$^{t}Bu$_3$-2,4,6))}$_2$][25] with $^2J_{^1H,^{89}Y}$ couplings between 2.3 and 3.0 Hz.

Small crystals of **2**·O(SiMe$_3$)$_2$ were obtained by cooling a concentrated O(SiMe$_3$)$_2$ solution to −30 °C, but the X-ray structure is only of suitable quality to establish connectivity (Figure 5). In the solid state, **2** adopts a distorted-octahedral geometry at yttrium with one methyl group of the AlMe$_4$ anion located in the plane of the NON donors of the XN$_2$ ligand, resulting in a more planar XN$_2$ ligand backbone relative to five-coordinate **1a**.

A range of rare-earth tetramethylaluminate complexes have previously been prepared by reaction of a metal alkyl or amido complex with a trialkylalane. However, in some cases these reactions resulted in multidentate ligand transfer from the rare-earth metal to aluminum, as illustrated in Scheme 3.[26] Furthermore, ligand transfer to aluminum has been observed in the reactions of several protio ligands or alkali-metal ligand salts with [Ln(AlMe$_4$)$_3$] reagents.[23,24,27] However, XN$_2$ ligand transfer to Al was not observed in the reaction to generate **2**,

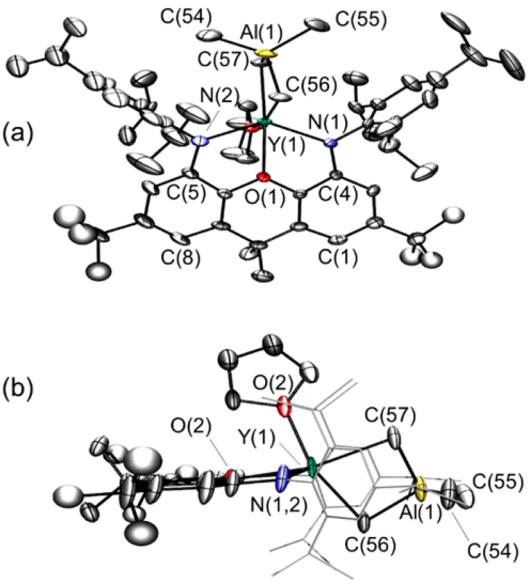

Figure 5. Two views of the X-ray crystal structure for [(XN$_2$)Y{(μ-Me)$_2$AlMe$_2$}(THF)]·O(SiMe$_3$)$_2$ (**2**·O(SiMe$_3$)$_2$). Ellipsoids are set to 50% probability. Hydrogen atoms and lattice solvent are omitted for clarity. The *tert*-butyl groups are rotationally disordered over two positions, and only one is shown for clarity. In (b) the 2,4,6-triisopropylphenyl groups are depicted in wire-frame format for clarity.

Scheme 3. Literature Reactions Involving Multidentate Ligand Transfer from a Rare-Earth Element to Aluminum

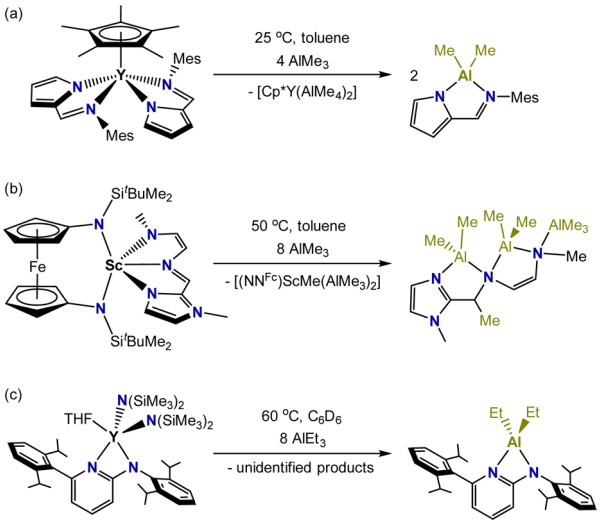

and compound **2** proved to be quite thermally robust, showing no sign of decomposition after heating at 80 °C in benzene for 24 h in the presence of excess AlMe$_3$. This lack of ligand transfer to aluminum is not due to an inability of the XN$_2$ ligand to accommodate aluminum, since [(XN$_2$)AlMe] (**3**) was accessible via the reaction of H$_2$XN$_2$ with AlMe$_3$ at 85 °C (Scheme 4).

X-ray-quality crystals of **3**·O(SiMe$_3$)$_2$ (Figure 6) were obtained by cooling a concentrated O(SiMe$_3$)$_2$ solution to −30 °C. Aluminum is four-coordinate with a significantly distorted trigonal planar arrangement of the three anionic donors; the sum of the N(1)−Al(1)−C(54), N(2)−Al(1)−C(54), and N(1)−Al(1)−N(2) angles is 355°, and C(54) is located 0.84 Å out of the N(1)/Al/N(2) plane. The neutral oxygen donor coordinates to aluminum with an obtuse O(1)−

DOI: 10.1021/acs.organomet.7b00156
Organometallics XXXX, XXX, XXX−XXX

Scheme 4. Alkane Elimination from $H_2[XN_2]$ and $AlMe_3$ To Form the Aluminum Methyl Complex $[(XN_2)AlMe]$ (3)

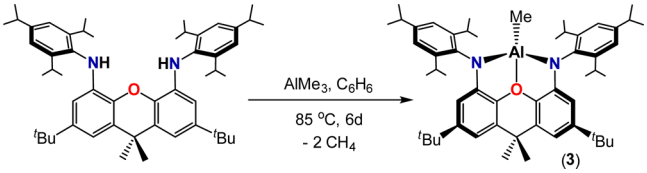

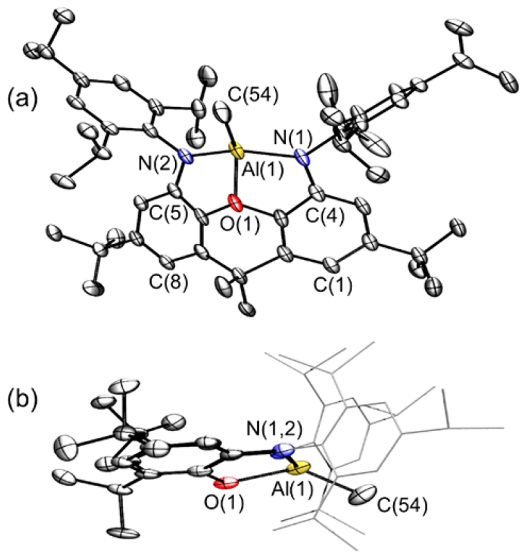

Figure 6. Two views of the X-ray crystal structure for $[(XN_2)AlMe]\cdot O(SiMe_3)_2$ ($3\cdot O(SiMe_3)_2$). Ellipsoids are set to 50% probability. Hydrogen atoms and lattice solvent are omitted for clarity. In view b the 2,4,6-triisopropylphenyl groups are depicted in wire-frame format for clarity. Selected bond lengths (Å) and angles (deg): Al−N(1) 1.858(2), Al−N(2) 1.871(2), Al−C(54) 1.942(2), Al−O(1) 1.973(2); N(1)−Al−N(2) 134.26(7), N(1)−Al−C(54) 110.77(9), N(2)−Al−C(54) 110.27(9), O(1)−Al−C(54) 134.80(9), O(1)−Al−N(1) 82.57(7), O(1)−Al−N(2) 82.73(7).

Al(1)−C(54) angle of 135°, but the Al(1)−O(1) distance of 1.973(2) Å is unremarkable. For example, it is only slightly longer than that in $[\{O(C_6H_4(NCy)\text{-}o)_2\}AlMe]$ (1.937(2) Å), in which the more flexible NON donor accommodates a more acute O−Al−C angle of 117.0(1)°,[28] and it is identical within error to the Al−O distance in $[\{(Me_3Si)_3C\}AlMe_2(THF)]$ (1.969(2) Å).[29]

The xanthene backbone of the XN_2 ligand in **3** is significantly bent, with a 47° angle between two aryl rings of the backbone (cf. 25° in **1a**), and aluminum is displaced 0.72 Å out of the NON plane. Furthermore, the amido donors of the XN_2 ligand are strongly bent toward aluminum, as illustrated by C(1)···C(8), C(4)···C(5), and N(1)···N(2) distances of 4.86, 4.20, and 3.44 Å. These structural features enable the XN_2 ligand to accommodate Al−N bonds in **3**, which are almost 0.4 Å shorter than the Y−N bonds in **1a** (1.858(2) and 1.871(2) Å for **3** vs 2.252(3) Å for **1a**). The Al−N distances in **3** are similar to those in four-coordinate $[\{O(C_6H_4(NCy)\text{-}o)_2\}AlMe]$ (1.837(2) and 1.854(2) Å,[28] and longer than those in three-coordinate $[\{ArN(CH_2)_3NAr\}AlMe]$ (Ar = $C_6H_3{}^iPr_2$-2,6; 1.760(3) and 1.766(3) Å).[30] This same trend is followed for the Al−C bonds, which are 1.942(2) Å in **3** and 1.947(3) Å[28] and 1.915(4) Å, respectively, for the aforementioned four- and three-coordinate literature complexes.[30]

The synthetic accessibility of both **1a** and **3** demonstrates the ability of the XN_2 ligand to accommodate both small and large metal ions, although this does not detract from the ability of 4,5-bis(anilido)xanthene dianions to function as rigid meridionally coordinating pincer ligands upon coordination to large rare-earth and actinide elements.[31]

Yttrium alkyl complex **1a** catalyzed intramolecular hydroamination of aminoalkenes in benzene at 24 °C (Table 1),

Table 1. Intramolecular Hydroamination Catalyzed by 1a (0.2 mol % (Entry 1), 1 mol % (Entry 2), or 10 mol % (Entries 3 and 4)) at 24 °C (unless Otherwise Specified) in C_6D_6

Entry	Substrate	Product	Time (h)	Conversion (%)[a]	N_t (h^{-1})[b]
1	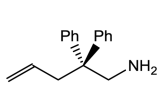	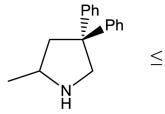	≤ 0.33	> 99%	≥1500
2	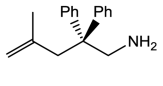	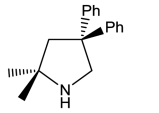	1.5	> 99%	~ 67
3	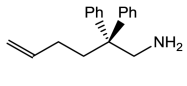	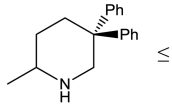	≤ 0.17	> 99%	≥ 60
4	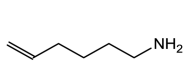		34 ≤ 0.75[c]	> 99% > 99%[c]	~ 0.3 ≥13[c]

[a]Percentage conversion to product relative to unreacted substrate, determined by ^{1}H NMR spectroscopy; [b]Turnover frequency; [c]60 °C.

leading to >99% product formation in all cases, as confirmed by ^{1}H NMR spectroscopy. The reaction with 1-amino-2,2-diphenyl-4-pentene (entry 1) was complete within 10 min with 1 mol % catalyst loading and within 20 min with 0.2 mol % of the catalyst. In contrast, the reactions with 1-amino-2,2-diphenyl-4-methyl-4-pentene (entry 2) and 1-amino-2,2-diphenyl-5-hexene (entry 3) required a longer reaction time or higher catalyst loading, respectively, for >99% conversion. The lower reactivity of these substrates is a consequence of increased alkene steric hindrance (entry 2 vs 1) and less favorable six- versus five-membered-ring formation (entry 3 vs 1). The room-temperature activity of **1a** for 1-amino-2,2-diphenyl-4-pentene hydroamination (TON ≥ 1500) is comparable to that of the most active rare-earth catalysts, including Hultzsch's yttrium catalysts in Figure 1 (Ar = $C_6H_3Me_2$-3,5)[4,32] and other group 3 and f-element catalysts reported by Marks ($[(^{Ph2}Box)LaR_2]$[33] and $[(CGC)AnR_2]$;[34] Box = 2,2′-bis(2-oxazoline)methylenyl; CGC = $Me_2Si(C_5Me_4)(N^tBu)$) and Schafer ($[(AI)YR_2(THF)]$; AI = $o\text{-}C_6H_4(NAr)(CH{=}NAr)$, Ar = $C_6H_3{}^iPr_2$-2,6).[35]

In comparison to 1-amino-2,2-diphenyl-5-hexene (Table 1, entry 3), cyclization of 1-amino-5-hexene (entry 4) required 10 mol % catalyst and an extended (34 h) reaction time for >99% conversion, due to the absence of cyclization-promoting geminal phenyl groups (Thorpe−Ingold effect).[36] The ability of **1a** to catalyze this reaction at room temperature is unusual, and at 60 °C the reaction was complete after 45 min,

DOI: 10.1021/acs.organomet.7b00156
Organometallics XXXX, XXX, XXX−XXX

corresponding to a turnover frequency (N_t) of 13 h^{-1}. For comparison, Marks' [$Cp^*_2La\{CH(SiMe_3)_2\}$][37] and [(CGC)-$Th(NMe_2)_2$][34] catalyzed 1-amino-5-hexene cyclization with turnover frequencies of 5 and 0.2 at 60 °C, respectively, and Hultzsch's yttrium binol catalyst (Figure 1b; Ar = $C_6H_3Me_2$-3,5) achieved a turnover frequency of 1.6 at 80 °C.[32]

At a catalyst loading of 10 mol %, compound **1a** catalyzed intermolecular hydroamination reactions utilizing 4-*tert*-butylaniline, 4-*tert*-butylbenzylamine, and *n*-octylamine in combination with 1-octene and diphenylacetylene (Table 2). These

Table 2. Intermolecular Hydroamination of 1-Octene (Entries 1−3) and Diphenylacetylene (Entries 4−6) Catalyzed by 1a (10 mol %) at 110 °C in Toluene

Entry[a]	Amine Substrate	Product[b,c]	Time (h)	Convers.[d] (%); Select.[e] (%)	N_t (h^{-1})[f]
1	Ar—NH_2	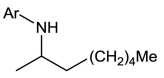	72 h	23; 97[h]	0.03
2		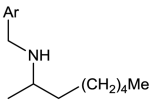	24 h	95; >99[i]	0.40
3	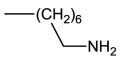	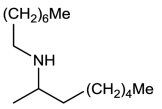	24 h	> 99; 96[h]	0.42
4	Ar—NH_2	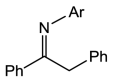	24 h	97[g]	0.40
5		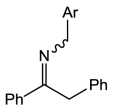	24 h	80[g]	0.33
6	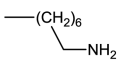	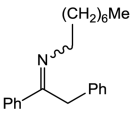	24h	> 99%[g]	0.42

[a]The alkene or alkyne reagent was present in 20-fold excess relative to the amine. [b]Ar = *p*-*tert*-butylphenyl. [c]The sole or major product in entries 4−6 is considered to be the *E* isomer, on the basis of literature assignments for similar compounds.[38] [d]Percentage conversion to product relative to unreacted amine substrate. [e]Selectivity for Markovnikov product formation. [f]Turnover frequency. [g]In entry 4, the product is formed as a single isomer, whereas in entries 5 and 6 it is formed as an 1:0.4 and 1:0.35 mixture of the *E* and *Z* isomers, respectively. [h]Selectivity determined by GC-MS. [i]Selectivity determined by ^{1}H NMR spectroscopy.

reactions were performed in toluene at 110 °C with a 20-fold excess of the alkene or alkyne substrate, and in all reactions with 1-octene the Markovnikov product was formed with high selectivity. Reactions with *n*-octylamine gave the highest conversion after 24 h, yielding >99% product with both 1-octene and diphenylacetylene (entries 3 and 6). Even with a shorter reaction time, the reaction of 1-octene with 4-*tert*-butylbenzylamine (entry 2) afforded a higher conversion to the hydroamination product than the reaction with 4-*tert*-butylaniline (entry 1), consistent with the reduced steric hindrance and unimpeded basicity of the former amine. In contrast, the turnover frequency for the analogous reactions with diphenylacetylene shows little variation among the three amine substrates (entries 4−6).[39]

SUMMARY AND CONCLUSIONS

In summary, a rigid NON-donor pincer ligand, XN_2, has been employed for the synthesis of two thermally robust yttrium alkyl complexes (**1a**,**b**), an yttrium tetramethylaluminate complex (**2**), and an aluminum methyl complex (**3**). The ability of XN_2 to accommodate both yttrium and aluminum demonstrates the versatility of the ligand for coordination to metal ions with very different radii. Compound **1a** was found to be highly active for both intra- and intermolecular hydroamination with a variety of substrates. The ability of **1a** to catalyze room-temperature intramolecular hydroamination of more challenging substrates (e.g., 1-amino-5-hexene) and intermolecular hydroamination of unactivated alkenes positions **1a** as one of the most active and general rare-earth hydroamination catalysts reported thus far.

EXPERIMENTAL SECTION

General Details. An argon-filled MBraun UNIlab glovebox equipped with a −30 °C freezer was employed for the manipulation and storage of all air-sensitive compounds, and reactions were performed on a double-manifold high-vacuum line using standard techniques.[40] A Fisher Scientific Ultrasonic FS-30 bath was used to sonicate reaction mixtures where indicated. A VWR Clinical 200 Large Capacity Centrifuge (with 28° fixed-angle rotors that hold 12 × 15 mL or 6 × 50 mL tubes) in combination with 15 mL Kimble Chase glass centrifuge tubes was used when required (inside the glovebox). Residual oxygen and moisture were removed from the argon stream by passage through an Oxisorb-W scrubber from Matheson Gas Products. Diethyl ether, THF, toluene, benzene, and hexanes were initially dried and distilled at atmospheric pressure from Na/Ph_2CO. Hexamethyldisiloxane ($O(SiMe_3)_2$) was dried and distilled at atmospheric pressure from Na. Unless otherwise noted, all protio solvents were stored over an appropriate drying agent (pentane, hexanes, and hexamethyldisiloxane over Na/Ph_2CO/tetra-glyme; Et_2O over Na/Ph_2CO) and introduced to reactions via vacuum transfer with condensation at −78 °C. The deuterated solvents (ACP Chemicals) C_6D_6, THF-d_8, and toluene-d_8 were dried over Na/Ph_2CO.

2,4,6-Triisopropylaniline,[14] 4,5-dibromo-2,7-di-*tert*-butyl-9,9-dimethylxanthene (XBr_2),[13] [$Y(CH_2SiMe_2R)_3(THF)_2$] (R = Me, Ph),[15] and the intramolecular hydroamination reagents[41] were prepared according to literature procedures. 1-Amino-5-hexene was purchased from GFS Chemicals, dried over CaH_2, and distilled prior to use. 1,3,5-Triisopropylbenzene, xanthone, KH (30 wt % in mineral oil), $LiCH_2SiMe_3$ (1.0 M in pentane), ^{n}BuLi (1.6 M in hexanes), Br_2, NaH, NaO^{t}Bu, $Pd(OAc)_2$, DPEPhos (bis{2-(diphenylphosphino)-phenyl} ether), diphenylacetylene, and $MgSO_4$ were purchased from Sigma-Aldrich. YCl_3 and $AlMe_3$ were purchased from Strem Chemicals. Solid $LiCH_2SiMe_3$ was obtained by removal of pentane in vacuo, and solid KH was obtained by filtration and washing with hexanes. [$YCl_3(THF)_{3.5}$] was obtained by refluxing the anhydrous YCl_3 in THF for 24 h followed by removal of the solvent in vacuo. 4-*tert*-Butylaniline, 4-*tert*-butylbenzylamine, *n*-octylamine, and 1-octene were purchased from Sigma-Aldrich, dried over molecular sieves, and distilled prior to use. Argon (99.999% purity) and ethylene (99.999% purity) were purchased from Praxair.

Combustion elemental analyses were performed both at McMaster University on a Thermo EA1112 CHNS/O analyzer and by Midwest Microlab, LLC, Indianapolis, IN, USA. NMR spectroscopy (^{1}H, $^{13}C\{^1H\}$, DEPT-Q, COSY, HSQC, HMBC) was performed on Bruker DRX-500 and AV-600 spectrometers. All ^{1}H NMR and ^{13}C NMR spectra were referenced relative to $SiMe_4$ through a resonance of the employed deuterated solvent or protio impurity of the solvent: C_6D_6 (7.16 ppm) and d_8-Tol (2.08, 6.97, 7.01, 7.09 ppm) for ^{1}H NMR; C_6D_6 (128.0 ppm) and d_8-Tol (20.43, 125.13, 127.96, 128.87, 137.48

DOI: 10.1021/acs.organomet.7b00156
Organometallics XXXX, XXX, XXX−XXX

ppm) for ^{13}C NMR. Herein, numbered proton and carbon atoms refer to the positions of the xanthene backbone, as shown in Scheme 1. Inequivalent *o*-isopropyl protons are labeled A and B, while inequivalent aryl ring protons and inequivalent methyl groups are labeled with ′ and ″, so that the corresponding carbon resonances can be identified. X-ray crystallographic analyses were performed on suitable crystals coated in Paratone oil and mounted on a SMART APEX II diffractometer with a 3 kW sealed-tube Mo generator in the McMaster Analytical X-ray (MAX) Diffraction Facility. In all cases, non-hydrogen atoms were refined anisotropically and hydrogen atoms were generated in ideal positions and then updated with each cycle of refinement.

GC-MS analyses were performed by Dr. Kirk Green and Dr. Fan Fei at the McMaster Regional Centre of Mass Spectrometry (MRCMS) using an Agilent 6890N gas chromatograph (Santa Clara, CA, USA), equipped with a DB-17ht column (30 m × 0.25 mm i.d. × 0.15 μm film, J & W Scientific) and a retention gap (deactivated fused silica, 5 m × 0.53 mm i.d.) and coupled to an Agilent 5973 MSD single-quadrupole mass spectrometer. A 1 μL portion of the sample was injected using the Agilent 7683 autosampler in splitless mode. The injector temperature was 230 °C, and the carrier gas (helium) flow was 0.7 mL/min. The transfer line was heated to 280 °C, and the MS source temperature was 230 °C. The column temperature started at 50 °C and was raised to 300 °C at 8 °C/min and held at 300 °C for 15 min for a total run time of 46.25 min. Full-scan mass spectra between *m*/*z* 50 and 800 were acquired after a 5 min solvent delay.

H_2XN_2. 4,5-Dibromo-2,7-di-*tert*-butyl-9,9-dimethylxanthene (5.0 g, 10.41 mmol), NaO^{t}Bu (2.8 g, 29.14 mmol), $Pd(OAc)_2$ (86.48 mg, 0.38 mmol), and DPEPhos (307.0 mg, 0.57 mmol) were dissolved in toluene (100 mL) followed by the addition of 2,4,6-triisopropylaniline (4.56 g, 20.8 mmol) via syringe. The reaction mixture was heated to 100 °C for 5 days, over which time a color change to chocolate brown was observed. The reaction mixture was then quenched with water, extracted into toluene (3 × 50 mL), dried over $MgSO_4$, filtered, and concentrated to approximately 10 mL. Recrystallization from hot ethanol yielded H_2XN_2 as an off-white solid (4.76 g, 60%). To remove excess moisture, the solid was stirred at room temperature with NaH (452 mg, 18.84 mmol) in toluene (35 mL) for 24 h followed by filtration, and concentration of the mother liquor yielded an off-white solid, which was then dissolved in hexanes (20 mL), centrifuged to remove a small amount of insoluble material, and evaporated to dryness in vacuo to yield H_2XN_2 as an off-white solid (4.08 g, 52% from starting materials). ^1H NMR (C_6D_6, 600 MHz): δ 7.25 (s, 4H, Ar-*H*), 6.98 (d, 2H, $^4J_{H,H}$ 2 Hz, Xanth-C*H*^{1}), 6.57 (d, 2H, $^4J_{H,H}$ 2 Hz, Xanth-C*H*^{3}), 5.90 (s, 2H, N*H*), 3.52 (sept, 4H, $^3J_{H,H}$ 7 Hz, *o*-C*H*Me$_2$), 2.86 (sept, 2H, $^3J_{H,H}$ 7 Hz, *p*-C*H*Me$_2$), 1.69 (s, 6H, C*Me*$_2$), 1.264 (d, 12H, $^3J_{H,H}$ 7 Hz, *o*-CH*Me*$_2$), 1.260 (d, 12H, $^3J_{H,H}$ 7 Hz, *p*-CH*Me*$_2$), 1.23 (s, 18H, C*Me*$_3$), 1.188 (d, 12H, $^3J_{H,H}$ 7 Hz, *o*-CH*Me*$_2$) ^{13}C NMR (C_6D_6, 126 MHz): δ 148.12 (*p*-CCHMe$_2$), 147.78 (Ar-C_{ipso}), 146.14 (Xanth-C^2), 136.56 (Xanth-C^{11}), 133.62 (*o*-CCHMe$_2$), 129.27 (Xanth-C^{10}), 122.15 (Ar-CH), 111.68 (Xanth-C^1H), 107.82 (Xanth-C^3H), 35.07 (Xanth-C^9 Me$_2$), 34.81 (*C*Me$_3$), 34.78 (*p*-CHMe$_2$), 32.96 (C*Me*$_2$), 31.71 (C*Me*$_3$), 28.89 (*o*-CHMe$_2$), 24.82 (*o*-CH*Me*$_2$), 24.41 (*p*-CH*Me*$_2$), 23.64 (*o*-CH*Me*$_2$). Anal. Calcd for $C_{53}H_{76}N_2O$: C, 84.06; H, 10.12; N, 3.69. Found: C, 83.88; H, 10.45; N, 3.28.

[(XN_2)Y(CH_2SiMe_3)(THF)]·*x*O$(SiMe_3)_2$ (1a·*x*O$(SiMe_3)_2$; *x* = 1–1.5). A solution of H_2XN_2 (0.150 g, 0.198 mmol) in benzene (5 mL) was added to [Y$(CH_2SiMe_3)_3(THF)_2$] (0.107 g, 0.217 mmol), and the solution was stirred for 24 h at 24 °C in the glovebox. Solvent was removed in vacuo, and the yellow solid was recrystallized from $O(SiMe_3)_2$ at −30 °C, yielding **1a**·*x*$O(SiMe_3)_2$ as a yellow solid (0.120 g, 52%). The amount of $O(SiMe_3)_2$ in samples of **1a** varied from 1.0 to 1.5; the sample used for elemental analysis contained 1.0 $O(SiMe_3)_2$ by NMR spectroscopy. ^1H NMR (C_6D_6, 600 MHz): δ 7.27 (s, 2H, Ar-*H*′), 7.14 (s, 2H, Ar-*H*″), 6.80 (d, 2H, $^4J_{H,H}$ 2 Hz, Xanth-C*H*^{1}), 6.23 (d, 2H, $^4J_{H,H}$ 2 Hz, Xanth-CH^3), 4.28 (sept, 2H, $^3J_{H,H}$ 7 Hz, A-*o*-C*H*Me$_2$), 3.32 (sept, 2H, $^3J_{H,H}$ 7 Hz, B-*o*-C*H*Me$_2$), 2.83 (sept, 2H, $^3J_{H,H}$ 7 Hz, para−C*H*Me$_2$), 2.68 (s, 4H, THF-$C^{2,5}H_2$), 1.89 (s, 3H, C*Me*$_2$′), 1.74 (s, 3H, C*Me*$_2$″), 1.50 (d, 6H, $^3J_{H,H}$ 7 Hz, A-*o*-CH*Me*$_2$′), 1.49 (d, 6H, $^3J_{H,H}$ 7 Hz, A-*o*-CH*Me*$_2$″), 1.27 (s, 18H, C*Me*$_3$), 1.12 (d, 6H, $^3J_{H,H}$ 7 Hz, B-*o*-CH*Me*$_2$′), 1.21 (d, 12H, $^3J_{H,H}$ 7 Hz, *p*-CH*Me*$_2$), 0.99 (d, 6H, $^3J_{H,H}$ 7 Hz, B-*o*-CH*Me*$_2$″), 0.84 (s, 4H, THF-$C^{3,4}H_2$), 0.36 (s, 9H, YCH$_2$Si*Me*$_3$), − 0.22 (d, 2H, $^2J_{Y,H}$ 3.6 Hz, YC*H*$_2$SiMe$_3$). ^{13}C NMR (C_6D_6, 126 MHz): δ 147.66 (Xanth-C_2), 147.21 (A-*o*-CCHMe$_2$), 146.33 (B-*o*-CCHMe$_2$), 145.34 (*p*-CCHMe$_2$), 141.33 (Xanth-C^{11}), 140.83 (Ar-C_{ipso}), 130.49 (Xanth-C^{10}), 122.23 (Ar-CH′), 121.90 (Ar-CH″), 108.68 (Xanth-C^3H), 106.52 (Xanth-C^1H), 70.27 (THF-$C^{2,5}H_2$), 35.57 (Xanth-C^9Me$_2$), 35.41 (*C*Me$_2$′), 35.03 (*C*Me$_3$), 34.52 (*p*-CHMe$_2$), 34.02 (d, $^1J_{Y,H}$ 51.12 Hz, YCH$_2$SiMe$_3$), 31.91 (C*Me*$_3$), 28.38 (B-*o*-CHMe$_2$), 27.90 (A-*o*-CHMe$_2$), 27.17 (A-*o*-CH*Me*$_2$″), 26.06 (B-*o*-CH*Me*$_2$″), 25.36 (B-*o*-CH*Me*$_2$′), 25.14 (C*Me*$_2$″), 24.90 (THF-$C^{3,4}H_2$), 24.60 (A-*o*-CH*Me*$_2$′), 24.49 (*p*-CH*Me*$_2$), 4.09 (YCH$_2$Si*Me*$_3$). Anal. Calcd for $C_{67}H_{111}N_2O_3YSi_3$: C, 69.02; H, 9.59; N, 2.40. Found: C, 68.61; H, 9.40; N, 2.82.

[(XN_2)Y(CH_2SiMe_2Ph)(THF)]·O$(SiMe_3)_2$ (1b·O$(SiMe_3)_2$). A solution of H_2XN_2 (0.100 g, 0.132 mmol) in benzene (7 mL) was added to [Y$(CH_2SiMe_2Ph)_3(THF)_2$] (0.098 g, 0.145 mmol), and the solution was stirred for 14 days in the glovebox at 24 °C. Solvent was removed in vacuo, and the dark yellow solid was recrystallized from $O(SiMe_3)_2$ at −30 °C, yielding **1b**·$O(SiMe_3)_2$ as a yellow-brown solid (0.079 g, 49%). ^1H NMR (C_6D_6, 600 MHz): δ 7.84 (m, 2H, YCH$_2$SiMe$_2$*Ph*), 7.22 (d, 2H, $^4J_{H,H}$ 1.68 Hz, Ar-*H*′), 7.20 (m, 3H, YCH$_2$SiMe$_2$*Ph*), 7.13 (d, 2H, $^4J_{H,H}$ 1.68 Hz, Ar-*H*″), 6.82 (d, 2H, $^4J_{H,H}$ 2 Hz, Xanth-C*H*^{3}), 6.23 (d, 2H, $^4J_{H,H}$ 2 Hz, Xanth-C*H*^{1}), 4.13 (sept, 2H, $^3J_{H,H}$ 7 Hz, A-*o*-C*H*Me$_2$), 3.34 (sept, 2H, $^3J_{H,H}$ 7 Hz, B-*o*-C*H*Me$_2$), 2.80 (sept, 2H, $^3J_{H,H}$ 7 Hz, *p*-C*H*Me$_2$), 2.66 (s, 4H, 1 equiv of THF-$2,5H_2$), 1.89 (s, 3H, C*Me*$_2$′), 1.73 (s, 3H, C*Me*$_2$″), 1.41 (d, 6H, $^3J_{H,H}$ 7 Hz, A-*o*-CH*Me*$_2$′), 1.34 (d, 6H, $^3J_{H,H}$ 7 Hz, A-*o*-CH*Me*$_2$″), 1.28 (s, 18H, C*Me*$_3$), 1.24 (d, 6H, $^3J_{H,H}$ 7 Hz, B-*o*-CH*Me*$_2$′), 1.18 (d, 12H, $^3J_{H,H}$ 7 Hz, *p*-CH*Me*$_2$), 1.00 (d, 6H, $^3J_{H,H}$ 7 Hz, B-*o*-CH*Me*$_2$″), 0.84 (s, 4H, THF-$C^{3,4}H_2$), 0.57 (s, 6H, YCH$_2$Si*Me*$_2$Ph), − 0.07 (d, 2H, $^2J_{Y,H}$3.6 Hz, YC*H*$_2$SiMe$_2$Ph). ^{13}C NMR (C_6D_6, 126 MHz): δ 147.79 (Xanth-C^2), 147.66 (A-*o*-CCHMe$_2$), 147.20 (YCH$_2$SiMe$_2$*Ph*$_{ipso}$), 146.19 (B-*o*-CCHMe$_2$), 145.40 (*p*-CCHMe$_2$), 141.23 (Xanth-C^{11}), 140.66 (Ar-C_{ipso}), 133.89 (YCH$_2$SiMe$_2$*Ph*), 130.46 (Xanth-C^{10}), 127.50 (YCH$_2$SiMe$_2$*Ph*), 122.28 (Ar-CH′), 121.87 (Ar-CH″), 108.77 (Xanth-C^1H), 106.72 (Xanth-C^3H), 70.37 (THF-$C^{2,5}H_2$), 35.59 (C*Me*$_2$′), 35.06 (Xanth-C^9Me$_2$), 34.87 (*C*Me$_3$), 34.50 (*p*-CHMe$_2$), 31.92 (C*Me*$_3$), 30.25 (YCH$_2$SiMe$_2$Ph), 28.42 (B-*o*-CHMe$_2$), 27.92 (A-*o*-CHMe$_2$), 27.19 (A-*o*-CH*Me*$_2$″), 26.06 (B-*o*-CH*Me*$_2$″), 25.41 (B-*o*-CH*Me*$_2$′), 25.20 (C*Me*$_2$″), 24.91 (THF-$C^{3,5}H_2$), 24.57 (A-*o*-CH*Me*$_2$′), 24.49 (*p*-CH*Me*$_2$), 2.39 (YCH$_2$Si*Me*$_2$Ph). Anal. Calcd for $C_{72}H_{113}N_2O_3YSi_3$: C, 70.43; H, 9.27; N, 2.28. Found: C, 70.28; H, 8.99; N, 2.29.

[(XN_2)Y$(\mu$-Me$)_2$AlMe$_2$(THF)]·O$(SiMe_3)_2$ (2·O$(SiMe_3)_2$). A solution of [(XN_2)Y(CH_2SiMe_3)(THF)]·$O(SiMe_3)_2$ (**1a**·$O(SiMe_3)_2$) in benzene (8 mL) was added to an excess of $AlMe_3$ (0.05 g, 0.686 mmol), and the resulting solution was stirred at 24 °C for 1 h. Solvent was removed in vacuo, and the yellow solid was recrystallized from $O(SiMe_3)_2$ at −30 °C, yielding **2**·$O(SiMe_3)_2$ as colorless crystals (0.008 g, 20%). Note: by ^1H NMR spectroscopy, compound **2** is formed cleanly in the reaction between **1a** and $AlMe_3$; thus, the low yield is due to losses during recrystallization. ^1H NMR (C_6D_6, 600 MHz): δ 7.23 (s, 4H, Ar-*H*), 6.81 (d, 2H, $^4J_{H,H}$ 2 Hz, Xanth-C*H*^{1}), 6.18 (d, 2H, $^4J_{Y,H}$ 2 Hz, Xanth-C*H*^{3}), 3.30 (sept, 4H, $^3J_{H,H}$ 7 Hz, *o*-C*H*Me$_2$), 3.29 (m, 4H, THF-$C^{2,5}H_2$), 2.83 (sept, 2H, $^3J_{H,H}$ 7 Hz, *p*-C*H*Me$_2$), 1.64 (s, 6H, C*Me*$_2$), 1.30 (d, 12H, $^3J_{H,H}$ 7 Hz, A-*o*-CH*Me*$_2$), 1.28 (d, 12H, $^3J_{H,H}$ 7 Hz, *p*-CH*Me*$_2$), 1.23 (s, 18H, C*Me*$_3$), 1.22 (d, 12H, $^3J_{H,H}$ 7 Hz, B-*o*-CH*Me*$_2$), 0.93 (m, 4H, THF-$C^{3,4}H_2$), − 0.56 (d, 12H, $^2J_{Y,H}$ 3.8 Hz, Al*Me*$_4$). ^{13}C NMR (C_6D_6, 126 MHz): δ 148.06 (Xanth-C^2), 146.84 (*p*-CCHMe$_2$), 146.25 (Xanth-C^4), 145.55 (*o*-CCHMe$_2$), 140.47 (Xanth-C^{11}), 138.05 (Ar-C_{ipso}), 129.81 (Xanth-C^{10}), 122.89 (Ar-CH), 109.56 (Xanth-C^3H), 108.78 (Xanth-C^1H), 70.11 (THF-$C^{2,5}H_2$), 35.07 (*C*Me$_3$), 35.04 (Xanth-C^9Me$_2$), 34.72 (*p*-CHMe$_2$), 31.79 (C*Me*$_3$), 31.46 (C*Me*$_2$), 29.43 (*o*-CHMe$_2$), 27.28 (B-*o*-CH*Me*$_2$), 24.83 (THF-$C^{3,4}H_2$), 24.39 (*p*-CH*Me*$_2$), 23.67 (A-*o*-CH*Me*$_2$), 3.22 (Al*Me*$_4$). Anal. Calcd for $C_{67}H_{112}N_2O_3YAlSi_2$: C, 69.03; H, 9.68; N, 2.41. Found: C, 68.51; H, 9.27; N, 2.53.

DOI: 10.1021/acs.organomet.7b00156
Organometallics XXXX, XXX, XXX−XXX

[(XN$_2$)AlCH$_3$]·O(SiMe$_3$)$_2$ (3·O(SiMe$_3$)$_2$). A solution of H_2XN_2 (0.05 g, 0.066 mmol) and $AlMe_3$ (0.007 g, 0.099 mmol) in benzene (3 mL) was then stirred at 85 °C in a sealed Schlenk flask for 6 days. Solvent was removed in vacuo, and the off-white solid was recrystallized from $O(SiMe_3)_2$ at −30 °C, yielding **3**·$O(SiMe_3)_2$ as colorless crystals (0.034 g, 54%). ^{1}H NMR (C_6D_6, 600 MHz): δ 7.27 (s, 4H, Ar-*H*), 6.75 (d, 2H, $^4J_{H,H}$ 2 Hz, Xanth-C*H*^{1}), 6.39 (d, 2H, $^4J_{H,H}$ 2 Hz, Xanth-C*H*^{3}), 3.58 (sept, 4H, $^3J_{H,H}$ 7 Hz, ortho−C*H*M e$_2$), 2.86 (sept, 2H, $^3J_{H,H}$ 7 Hz, para−C*H*Me$_2$), 1.58 (s, 6H, C*Me*$_2$), 1.36 (d, 12H, $^3J_{H,H}$ 7 Hz, A-*o*-CH*Me*$_2$), 1.26 (d, 12H, $^3J_{H,H}$ 7 Hz, *p*-CH*Me*$_2$), 1.20 (d, 12H, $^3J_{H,H}$ 7 Hz, B-*o*-CH*Me*$_2$), 1.18 (s, 18H, C*Me*$_3$), −0.36 (s, 3H, Al*Me*). ^{13}C NMR (C_6D_6, 126 MHz): δ 149.45 (Xanth-C^2), 146.88 (*o*-CCHMe$_2$), 146.36 (*p*-CCHMe$_2$), 143.73 (Xanth-C^4), 141.83 (Xanth-C^{11}), 138.38 (Ar-C$_{ipso}$), 133.82 (Xanth-C^{10}), 122.31 (Ar-CH), 111.42 (Xanth-C^{3}H), 107.74 (Xanth-C^{1}H), 37.58 (Xanth-C^9 Me$_2$), 35.18 (CMe$_3$), 34.53 (*p*-CHMe$_2$), 31.72 (C*Me*$_3$), 29.20 (*o*-CHMe$_2$), 27.33 (C*Me*$_2$), 26.00 (B-*o*-CH*Me*$_2$), 24.57 (A-*o*-CH*Me*$_2$), 24.36 (*p*-CH*Me*$_2$), −12.74 (Al*Me*). Anal. Calcd for $C_{60}H_{95}N_2O_2AlSi_2$: C, 75.10; H, 9.98; N, 2.92. Found: C, 75.12; H, 9.78; N, 2.92.

General Procedure for Intramolecular Hydroamination. In the glovebox, the appropriate amounts of **1a**·$O(SiMe_3)_2$ and the hydroamination substrate were weighed into separate vials, dissolved in C_6D_6, and placed in a Teflon-valved J. Young NMR tube. The reactions were monitored at 24 °C by ^{1}H NMR spectroscopy, and products were identified by comparison to literature spectra.[41]

General Procedure for Intermolecular Hydroamination. In the glovebox, the appropriate amounts of **1a**·$O(SiMe_3)_2$, the amine, and the alkene/alkyne were weighed into separate vials, dissolved in d_8-toluene, placed in a Teflon-valved J. Young NMR tube and then placed into a preheated oil bath at 110 °C. After heating for the designated amount of time, NMR spectra were obtained and the sample was submitted for GC-MS analysis.

■ ASSOCIATED CONTENT

Supporting Information

The Supporting Information is available free of charge on the ACS Publications website at DOI: 10.1021/acs.organomet.7b00156.

NMR spectra for new compounds and NMR or mass spectra for hydroamination reaction products (PDF)

Crystallographic data (CIF)

■ AUTHOR INFORMATION

Corresponding Author

*D.J.H.E.: tel, 905-525-9140; fax, 905-522-5209; e-mail, emslied@mcmaster.ca.

ORCID

David J. H. Emslie: 0000-0002-2570-9345

Notes

The authors declare no competing financial interest.

■ ACKNOWLEDGMENTS

D.J.H.E. thanks the NSERC of Canada for a Discovery Grant and an NSERC Strategic Grant in collaboration with NOVA Chemicals. K.S.A.M. thanks the Government of Ontario for an OGS-Queen Elizabeth II Graduate Scholarship in Science and Technology (QEII GSST) scholarship. The authors thank Dr. Kirk Green and Dr. Fan Fei from the McMaster Regional Centre of Mass Spectrometry (MRCMS) for MS operation and assistance with the analysis of all the MS samples.

■ REFERENCES

(1) (a) Trifonov, A. A.; Basalov, I. V.; Kissel, A. A. *Dalton Trans.* **2016**, *45*, 19172. (b) Reznichenko, A. L.; Hultzsch, K. C. *Top. Organomet. Chem.* **2011**, *43*, 51. (c) Müller, T. E.; Hultzsch, K. C.; Yus, M.; Foubelo, F.; Tada, M. *Chem. Rev.* **2008**, *108*, 3795. (d) Hong, S.; Marks, T. J. *Acc. Chem. Res.* **2004**, *37*, 673.

(2) (a) Ryu, J. S.; Li, G. Y.; Marks, T. J. *J. Am. Chem. Soc.* **2003**, *125*, 12584. (b) Li, Y. W.; Marks, T. J. *Organometallics* **1996**, *15*, 3770.

(3) Reznichenko, A. L.; Nguyen, H. N.; Hultzsch, K. C. *Angew. Chem., Int. Ed.* **2010**, *49*, 8984.

(4) Reznichenko, A. L.; Hultzsch, K. C. *Organometallics* **2013**, *32*, 1394.

(5) Gromada, J.; Carpentier, J. F.; Mortreux, A. *Coord. Chem. Rev.* **2004**, *248*, 397.

(6) (a) Gibson, V. C.; Spitzmesser, S. K. *Chem. Rev.* **2003**, *103*, 283. (b) Nishiura, M.; Hou, Z. M. *Nat. Chem.* **2010**, *2*, 257.

(7) (a) Fridrichova, A.; Varga, V.; Pinkas, J.; Lamac, M.; Ruzicka, A.; Horacek, M. *Eur. J. Inorg. Chem.* **2016**, *2016*, 3713. (b) Ihara, E.; Yoshioka, S.; Furo, M.; Katsura, K.; Yasuda, H.; Mohri, S.; Kanehisa, N.; Kai, Y. *Organometallics* **2001**, *20*, 1752.

(8) Korobkov, I.; Gambarotta, S. *Organometallics* **2009**, *28*, 4009.

(9) Seyam, A. M.; Stubbert, B. D.; Jensen, T. R.; O'Donnell, J. J.; Stern, C. L.; Marks, T. J. *Inorg. Chim. Acta* **2004**, *357*, 4029.

(10) Cruz, C. A.; Emslie, D. J. H.; Harrington, L. E.; Britten, J. F.; Robertson, C. M. *Organometallics* **2007**, *26*, 692.

(11) Andreychuk, N. R.; Ilango, S.; Vidjayacoumar, B.; Emslie, D. J. H.; Jenkins, H. A. *Organometallics* **2013**, *32*, 1466.

(12) (a) Cruz, C. A.; Emslie, D. J. H.; Harrington, L. E.; Britten, J. F. *Organometallics* **2008**, *27*, 15. (b) Cruz, C. A.; Emslie, D. J. H.; Robertson, C. M.; Harrington, L. E.; Jenkins, H. A.; Britten, J. F. *Organometallics* **2009**, *28*, 1891.

(13) Nowick, J. S.; Ballester, P.; Ebmeyer, F.; Rebek, J. *J. Am. Chem. Soc.* **1990**, *112*, 8902.

(14) (a) Newton, A. *J. Am. Chem. Soc.* **1943**, *65*, 2434. (b) Liu, J.-Y.; Zheng, Y.; Li, Y.-G.; Pan, L.; Li, Y.-S.; Hu, N.-H. *J. Organomet. Chem.* **2005**, *690*, 1233. (c) Liu, J.; Li, Y.; Li, Y.; Hu, N. *J. Appl. Polym. Sci.* **2008**, *109*, 700.

(15) (a) Estler, F.; Eickerling, G.; Herdtweck, E.; Anwander, R. *Organometallics* **2003**, *22*, 1212. (b) Emslie, D. J. H.; Piers, W. E.; Parvez, M.; McDonald, R. *Organometallics* **2002**, *21*, 4226.

(16) Piers, W. E.; Emslie, D. J. H. *Coord. Chem. Rev.* **2002**, *233-234*, 131.

(17) Graf, D. D.; Davis, W. M.; Schrock, R. R. *Organometallics* **1998**, *17*, 5820.

(18) Chapurina, Y.; Guillot, R.; Lyubov, D.; Trifonov, A.; Hannedouche, J.; Schulz, E. *Dalton Trans.* **2013**, *42*, 507.

(19) Avent, A. G.; Cloke, F. G. N.; Elvidge, B. R.; Hitchcock, P. B. *Dalton Trans.* **2004**, 1083.

(20) Kissel, A. A.; Mahrova, T. V.; Lyubov, D. M.; Cherkasov, A. V.; Fukin, G. K.; Trifonov, A. A.; Del Rosal, I.; Maron, L. *Dalton Trans.* **2015**, *44*, 12137.

(21) Lu, E. L.; Gan, W.; Chen, Y. F. *Organometallics* **2009**, *28*, 2318.

(22) Hamidi, S.; Jende, L. N.; Dietrich, H. M.; Maichle-Mossmer, C.; Tornroos, K. W.; Deacon, G. B.; Junk, P. C.; Anwander, R. *Organometallics* **2013**, *32*, 1209.

(23) Litlabo, R.; Lee, H. S.; Niemeyer, M.; Tornroos, K. W.; Anwander, R. *Dalton Trans.* **2010**, *39*, 6815.

(24) Zimmermann, M.; Estler, F.; Herdtweck, E.; Tornroos, K. W.; Anwander, R. *Organometallics* **2007**, *26*, 6029.

(25) Schadle, D.; Schadle, C.; Tornroos, K. W.; Anwander, R. *Organometallics* **2012**, *31*, 5101.

(26) (a) Kaneko, H.; Dietrich, H. M.; Schadle, C.; Maichle-Mossmer, C.; Tsurugi, H.; Tornroos, K. W.; Mashima, K.; Anwander, R. *Organometallics* **2013**, *32*, 1199. (b) Huang, W. L.; Carver, C. T.; Diaconescu, P. L. *Inorg. Chem.* **2011**, *50*, 978. (c) Doring, C.; Kempe, R. *Eur. J. Inorg. Chem.* **2009**, *2009*, 412.

(27) (a) Zimmermann, M.; Tornroos, K. W.; Anwander, R. *Angew. Chem., Int. Ed.* **2008**, *47*, 775. (b) Zimmermann, M.; Takats, J.; Kiel, G.; Tornroos, K. W.; Anwander, R. *Chem. Commun.* **2008**, 612.

(28) Hild, F.; Neehaul, N.; Bier, F.; Wirsum, M.; Gourlaouen, C.; Dagorne, S. *Organometallics* **2013**, *32*, 587.

(29) Schnitter, C.; Roesky, H. W.; Albers, T.; Schmidt, H.; Ropken, C.; Parisini, E.; Sheldrick, G. M. *Chem. - Eur. J.* **1997**, *3*, 1783.

DOI: 10.1021/acs.organomet.7b00156
Organometallics XXXX, XXX, XXX−XXX

(30) Chakraborty, D.; Chen, E. Y. X. *Organometallics* **2002**, *21*, 1438.
(31) The closely related XA_2 ligand has also been coordinated to large Th(IV), U(IV), and U(III) centers, as well as much smaller Mg(II), and related *N*-mesityl- and *N*-cyclohexyl-substituted 4,5-bis(amido)xanthene ligands were coordinated to Ti(IV): (a) References 10−12.. (b) Cruz, C. A.; Chu, T.; Emslie, D. J. H.; Jenkins, H. A.; Harrington, L. E.; Britten, J. F. *J. Organomet. Chem.* **2010**, *695*, 2798. (c) Cruz, C. A.; Emslie, D. J. H.; Jenkins, H. A.; Britten, J. F. *Dalton Trans.* **2010**, *39*, 6626. (d) Vidjayacoumar, B.; Ilango, S.; Ray, M. J.; Chu, T.; Kolpin, K. B.; Andreychuk, N. R.; Cruz, C. A.; Emslie, D. J. H.; Jenkins, H. A.; Britten, J. F. *Dalton Trans.* **2012**, *41*, 8175. (e) Porter, R. M.; Danopoulos, A. A. *Polyhedron* **2006**, *25*, 859.
(32) Gribkov, D. V.; Hultzsch, K. C.; Hampel, F. *J. Am. Chem. Soc.* **2006**, *128*, 3748.
(33) Hong, S. W.; Tian, S.; Metz, M. V.; Marks, T. J. *J. Am. Chem. Soc.* **2003**, *125*, 14768.
(34) Stubbert, B. D.; Marks, T. J. *J. Am. Chem. Soc.* **2007**, *129*, 4253.
(35) Lauterwasser, F.; Hayes, P. G.; Piers, W. E.; Schafer, L. L.; Brase, S. *Adv. Synth. Catal.* **2011**, *353*, 1384.
(36) (a) Beesley, R. M.; Ingold, C. K.; Thorpe, J. F. *J. Chem. Soc., Trans.* **1915**, *107*, 1080. (b) Jung, M. E.; Piizzi, G. *Chem. Rev.* **2005**, *105*, 1735.
(37) Gagne, M. R.; Stern, C. L.; Marks, T. J. *J. Am. Chem. Soc.* **1992**, *114*, 275.
(38) (a) Ahlbrecht, H.; Fischer, S. *Tetrahedron* **1970**, *26*, 2837. (b) Tonks, I. A.; Meier, J. C.; Bercaw, J. E. *Organometallics* **2013**, *32*, 3451.
(39) The rate-determining step for alkene and alkyne hydroamination is typically considered to be insertion. However, whereas the insertion reaction for alkenes is approximately thermoneutral, it is strongly exothermic for alkynes, and some results suggest that in the case of alkynes (as well as dienes and allenes) the rate-determining step for certain catalysts may be protonolysis: Reznichenko, A. L.; Hultzsch, K. C. *Top. Organomet. Chem.* **2011**, *43*, 51.
(40) Burger, B. J.; Bercaw, J. E. Vacuum Line Techniques for Handling Air-Sensitive Organometallic Compounds. In *Experimental Organometallic Chemistry: A Practicum in Synthesis and Characterization*; Wayda, A. L., Darensbourg, M. Y., Eds.; American Chemical Society: Washington DC, 1987; ACS Symposium Series *357*, pp 79−98.
(41) Crimmin, M. R.; Arrowsmith, M.; Barrett, A. G. M.; Casely, I. J.; Hill, M. S.; Procopiou, P. A. *J. Am. Chem. Soc.* **2009**, *131*, 9670. See the Supporting Information for additional details.

DOI: 10.1021/acs.organomet.7b00156
Organometallics XXXX, XXX, XXX−XXX